Advances in Science and Technology Research Journal

*Advances in Science and Technology Research Journal*, 2025, 19(3), 283–298
https://doi.org/10.12913/22998624/199584
ISSN 2299-8624, License CC-BY 4.0

Received: 2024.10.23
Accepted: 2025.01.14
Published: 2025.02.01

# Mechanical properties of 3D-printed polylactide and short carbon fibres reinforced polylactide laminate subjected to environmental aging

Angela Jadwiga Andrzejewska-Sroka[1*], Magdalena Rucka[1]

[1] Department of Mechanics of Materials and Structures, Faculty of Civil and Environmental Engineering, Gdansk University of Technology, ul. Narutowicza 11/12, 80-233 Gdansk, Poland
* Corresponding author's e-mail: angela.andrzejewska@pg.edu.pl

## ABSTRACT

In this work, the mechanical characterisation of fused filament fabricated non-reinforced polylactide and polylactide reinforced with short carbon fibre laminate after environmental aging was reported. In the manufacturing process, the symmetric laminate was used to determine the influence of environmental aging of the 3D printed parts. The sterilisation agents and buffered saline solution environment were used as aging factors. Also, the fracture surfaces of non-reinforced and reinforced specimens were imaged with scanning electron microscopy. It was found that short carbon fibres in general influence the higher mechanical strength of materials, compared to materials without fibres. However, at the same time the addition of short carbon fibre contributes to a significant loss of toughness when aged with sterilisation agents and buffered saline solution environment over one, six or twelve weeks. The results presented in this work are important for several reasons. The study highlights how the addition of short carbon fibres enhances the mechanical properties of polylactide (PLA), which is valuable for the applications requiring increased strength and stiffness, while also addressing the impact of environmental aging, particularly in sterilisation and buffered saline solution environment. This is crucial in understanding the mechanical behaviour of these materials, as many PLA applications (e.g., in medical devices or marine environments) involve the exposure to conditions like mentioned above. Understanding how aging affects the mechanical properties of a material helps project lifetime and reliability of products.

**Keywords:** composite material filament, additive manufacturing, water environment aging, sterilisation, sustainable manufacturing.

## INTRODUCTION

### Mechanical properties of additive manufacturing materials

Additive manufacturing of engineering components with thermoplastic polymers is extensively practiced in the medical, automotive, or aerospace industries. The manufactured parts becoming a substitute for those produced by traditional manufacturing technologies. Unfortunately, there are some inconveniences associated with layer-by-layer printing of composite materials, which may contribute to the deterioration of their mechanical properties. In general, the structure of inner layers of additive manufactured parts is associated with printing orientation on the printing plane [1]. There are three main build directions: flat, on edge and upright. Hanon et al. [2] noted that flat and on-edge specimens revealed a major plastic behaviour. This is a consequence of arrangement of filament in the same direction to the pulling direction of specimen. Hence, contour and raster are longitudinally pulled. However, when using upright specimen, its fracture fragile because and not much plastic deformation was observed. This behaviour is related to tension load during the test, which was applied perpendicular to the built layers, and the bonding strength between the layers is weaker than the resistance of pulled contours.

In addition, the presence of voids causes microporous structures in printed parts, which reduces tensile strength. In their work, Tao et al. [3] highlighted five categories of voids, which vary in the mechanism of their formation: raster voids, partial neck growth voids, voids below the perimeter, voids inside the beads, and filling voids. Also, Yao et al. [4] proved that the tensile strength increases along with the printing angle of inclination of the print wall from the vertical axis or the decrease of the layer thickness.

In particular cases, through careful selection of fabrication parameters, such as in-plane build direction, temperature or printing speed, resulting in voids reduction or delamination between layers, it is not possible to achieve the desired strength or stiffness. For this reason, it is necessary to use the materials that contain the additives that improve their mechanic behaviour, such as carbon fibre, microcrystalline cellulose, core-shell rubber, wood, basalt fibres.

In the field of additive manufacturing with fibre fillers, the continuous [5–6] or short fibre [7–8] may be used. The carbon fibre features good strength-to-weight ratio and stiffness. When added to a polymer matrix in additive manufacturing process, it can significantly enhance the mechanical properties of the resulting composite. With its use, it can be possible to increase tensile strength, flexural strength, or impact resistance. In the commercial distribution, several popular filaments can be bought with short carbon fibre fill including PLA, polyethylene terephthalate glycol-modified (PETG), nylon, acrylonitrile butadiene styrene (ABS), and polycarbonate.

## Additive manufactured parts as a laminates

The term "laminate" is applicable to 3D-printed elements created via the Fused Filament Fabrication (FFF) method due to the fundamental characteristics of the printing process, which involves layer-by-layer deposition. In FFF, thermoplastic filament is extruded and laid down in successive layers that fuse together to form a solid object.

Each of these layers can be considered a "laminate," as the material is built up in thin, discrete layers, much like traditional composite laminates, where multiple layers of material are stacked and bonded to create a structure with enhanced mechanical properties [9].

The fabrication of 3D-printed objects and traditional laminated composite materials, such as fiberglass laminates, share a fundamental similarity in their underlying construction [10]. Both are composed of individual layers of materials that are bonded together to form a cohesive and integrated structure. This layered approach is crucial for imparting the desired mechanical properties, as each individual layer contributes to the overall strength, stiffness, and durability of the final product. The interlayer adhesion, whether in 3D-printed parts or traditional composites, is a key factor in determining the integrity and performance of the assembled structure. Ensuring strong bonding between these layers is essential for transferring loads effectively and maintaining the structural integrity of the final component.

The layered construction of objects produced via Fused Filament Fabrication 3D printing closely resembles the architecture of traditional laminated composite materials. This analogous structural design results in printed parts exhibiting mechanical properties akin to those observed in laminated composites. Consequently, the term "laminate" suitably describes the printed structures, as it encapsulates the fundamental layered nature of the 3D-printed parts and the crucial role of interlayer bonding in determining their overall performance [11–12].

Similar to how fibre orientations in composite laminates optimise strength, FFF printing enables precise control over layer deposition, allowing for the tailoring of specific mechanical and functional characteristics. This customisation capacity is a key advantage shared by both traditional laminates and modern 3D-printed materials [13].

However, the interlayer bonding in FFF-printed parts can be challenging to achieve, often resulting in delamination and reduced mechanical integrity compared to traditional manufacturing methods [14].

## Environmental aging of additive manufacturing materials

Environmental aging is the process when materials degrade and change their properties occur over time due to exposure to various environmental factors. In materials used in additive manufacturing, the environmental aging factors can have significant implications for their performance and durability. The most important factors regarding the environmental aging of these materials include: exposure to moisture or humidity [15–18],

UV radiation [18–20], heat [16, 18] or exposure to chemical agents [21–22].

When the thermoplastic biodegradable materials like PLA are used in 3D printing, the common issue is moisture absorption. The problem with moisture absorption can be considered in two ways. The first way is air moisture absorption associated with filament storage used in 3D printing, but the second way is humidity or moisture of working environment, for example, working in marine environments [23–24] or for biological [15, 17] use. Consequently, exposure to humidity or moisture can lead to changes in material properties, such as reduced strength, increased brittleness, and warping or it can also affect the adhesion of layers during printing. Also, the exposure of extreme temperatures, both high or low, during printing process or post-processing might affect the dimensional stability of 3D printed parts. The temperature during printing is considered an external factor, like, for example, the ambient temperature. That is, if the temperature rises or reduces rapidly during printing, damage to the print layers can occur. Its thermal expansion and contraction can result in warping, delamination, or cracking. Some materials are more sensitive to temperature changes than others, and it is related to melting temperature, glass transition temperature or softening point. It is therefore advantageous to use equipment with closed printing chambers that maintain a constant printing temperature. This is in contrast to open systems, where users sometimes place cardboard over the device to eliminate ambient temperature fluctuations.

Polylactide (PLA) and its composites are widely employed in biomedical devices, implants, and tissue engineering applications due to their excellent biocompatibility and biodegradability. To ensure these materials are free of contaminants, effective sterilisation is essential. Sterilisation methods, such as gas plasma (VH2O2) and ethylene oxide (EtO) sterilisation are preferred for their compatibility with sensitive materials. Gas plasma sterilisation operates at low temperatures using reactive gas plasma, which minimises thermal degradation of the material. In contrast, ethylene oxide sterilisation, effectively penetrates complex geometries, making it particularly suitable for 3D-printed structures. Furthermore, it does not require moisture, preserving the integrity of PLA and PLA-carbon fibre composites.

## Effect of carbon fibre on tensile properties of environmental aged biodegradable material

In a comparison between dry PLA and PLA+CF specimens, it was observed that the addition of carbon fibres enhances the tensile properties of symmetric composites with a raster orientation of +45°/-45°. This finding aligns with the observations described in [28], despite differences in raw materials and process parameters. Furthermore, the inclusion of carbon fibres in the polylactide matrix significantly improves mechanical characteristics, a phenomenon influenced by infill directions [24]. When a layer is deposited perpendicular to the zero axis, the polymer chains may entangle around the carbon fibres in the lower layer. This entanglement could improve Young's modulus by reinforcing the bond between layers, as described in previous studies [26–28].

The introduction of additional aging factors resulted in changes to the tensile properties of the materials. It was observed that pure PLA exhibited higher toughness values in week 6 (W6) and week 12 (W12) compared to the specimens reinforced with carbon fibres when aged in a buffered saline solution environment or subjected to both sterilisation agents and buffered saline solution aging. The reduction in strength observed in composite laminates aged under the conditions of water absorption can be attributed to the limitations on matrix deformation imposed by the fibres, as described in [28] [2].

This phenomenon has been widely studied in the literature, where fibre-matrix interactions are identified as a critical factor influencing the ultimate mechanical performance of composite materials under tensile loading. The constraints imposed by fibres can restrict the ability of the matrix to deform and transfer stress effectively, leading to reductions in composite strength and energy absorption behaviour. These findings underscore the importance of understanding the complex interactions between fibres and matrix components to optimise the performance and durability of fibre-reinforced composites, particularly under challenging environmental conditions [28].

Additionally, aging with sterilisation agents and exposure to temperatures near the glass transition temperature can significantly affect material behaviour. As aging time increases, molecules from the buffered saline solution occupy additional volume within the PLA+CF composite, contributing to its brittle characteristics [29].

Moreover, moisture absorption in natural fibres impacts laminates in several ways, including wear rate, crack propagation, and surface reactions during sliding, as reported in [30]. Water absorption affects natural fibres in two stages: initially causing the fibres to swell, followed by changes in fibre density corresponding to the weight of the absorbed moisture [31].

Water can significantly affect carbon fibre materials, especially when used in composite forms where carbon fibres are embedded in a polymer matrix. The impact of water on carbon fibre materials is typically indirect, as the carbon fibres themselves are chemically inert and hydrophobic. However, the matrix material and the fibre-matrix interface are more susceptible to water-related degradation. Water can infiltrate the interface between carbon fibres and the matrix, reducing adhesion and weakening the ability of the composite to transfer stress from the matrix to the fibres [32].

### Motivation and objective

The literature review proves that in development and future application of additive manufacturing parts with thermoplastic materials requires the proper manufacturing, postprocessing and working conditions. In some cases, it is crucial to improve the mechanical properties of 3D printed materials, with additives. Also, several factors, such as exposure to moisture or humidity, UV radiation, heat or exposure to chemicals, can affect the changes in mechanical properties.

To the best authors' knowledge, there is no study considered environmental aging of the interface for additive manufacturing biodegradable materials reinforced with short carbon fibre. The quantities of interest are tensile properties of symmetric laminates manufactured with pure or reinforced with short carbon fibre polylactide and it were aged in a buffered saline solution environment and/or with sterilisation agents.

The objective of this work was to experimentally characterise the changes in mechanical properties during environmental aging of a pure PLA material without any dyes and reinforcement additives and its comparison with black polylactide with short carbon fibres reinforcement (PLA+CF). The environmental aging factors, such as buffered saline solution environment (PBS) at 37 °C, sterilisation with ethylene oxide (EtO) or gas plasma (VH2O2) were used.

For this purpose, specially oriented 3D-printed symmetric laminate with 0.2 mm layer height was prepared and being tested up to failure. The laminate prepared in this way are novel for the study of additive manufactured materials. The research presented in the scientific literature focuses in general on asymmetric laminates. After the mechanical testing, scanning electron microscopy (SEM) technique were used in analysis of fracture surfaces. The micrographs provided information regarding the raster orientation, voids or carbon fibre orientation.

In the case of manufacturing composites by traditional methods, a basic and important property of all symmetric fibre-reinforced composites, regardless of their further characteristics, is that the interfacial coupling stiffness matrix is a zero matrix. This means that bending-stretch coupling, tensile-shear coupling and bending-torsional coupling are negligible, reflecting the separation of in-plane and out-of-plane deformation modes [33]. This attribute of a matrix with zero coupling stiffness in symmetric fibre-reinforced laminate composites produced using traditional methods has important implications. In particular, it ensures that symmetric laminates do not incline to buckle during the curing process after lamination. As a result, the separation of in-plane and out-of-plane deformation modes prevents the introduction of destabilizing coupling effects that could lead to unwanted buckling. This fundamental feature of traditional composite manufacturing is critical to ensuring the structural integrity and dimensional stability of the final composite component, especially during the critical curing stage, where residual stresses can develop [34]. Keeping this separation of deformation modes is an important design feature for engineers developing symmetric fibre-reinforced composite laminates and this phenomenon was adapted to additive manufactured materials.

## EXPERIMENTAL INVESTIGATIONS

### Object of research

In this paper, two types of polylactide (PLA) filament were selected for the study. Polylactide is a commonly used 3D printing material with biodegradable properties. In turn, addition of carbon fibre to polymer matrix offer greater stiffness and strength of the composite. In the study,

pure neutral polylactide and polylactide filled with short carbon fibre were used. These materials were produced by 3DXTECH (Grand Rapids, MI, USA), and it was: ECOMAX® PLA made using Natureworks 4043D PLA biopolymer and CarbonX™ PLA+CF made using Natureworks PLA and 100% premium recycled carbon fibre. The content of carbon fibres was 20% by weight, while their diameter was 5–10 micrometres.

The "dog bone" shaped specimens with measurement base length and width of 60 mm and 20 mm, respectively, were used, as shown in Figure 1. The nominal thickness was 3.6 mm, reached with 18 printed layers the stacking sequence of which was [+45°/-45°], but layer no. 9 and 10 had the same raster alignment angle [+45°] to ensure the symmetry of laminate. In each testing group, five specimens were used. A total of 60 specimens were examined in the PLA specimen group and 60 specimens in the PLA+CF specimen group.

The test specimens were shaped with fused FFF with CREALITY Ender 6X (Shenzhen, China), customised by using hardened steel nozzle with 0.8 mm diameter, and maximum temperatures of extrusion or cooling. The most important processing parameters generated in Simplify3D software were: extrusion multiplier – 1; extrusion width – 0.8 mm; primary layer height – 0.2 mm; top/bottom solid layers – 0; outline/perimeter shells – 1; outline direction – outside-in; internal/external fill pattern – rectilinear; build direction – flat; interior fill percentage – 100%; extruder temperature – 205 ± 1 °C; heated bed temperature – 60 ± 1 °C; default printing speed – 3000 mm/min.

## Experimental setup and procedure

Testing procedure was realised in four testing paths, using samples made of pure polylactide (PLA) or polylactide with short carbon fibres reinforcement (PLA+CF). In path 1, PLA and PLA+CF specimens were measured to determine

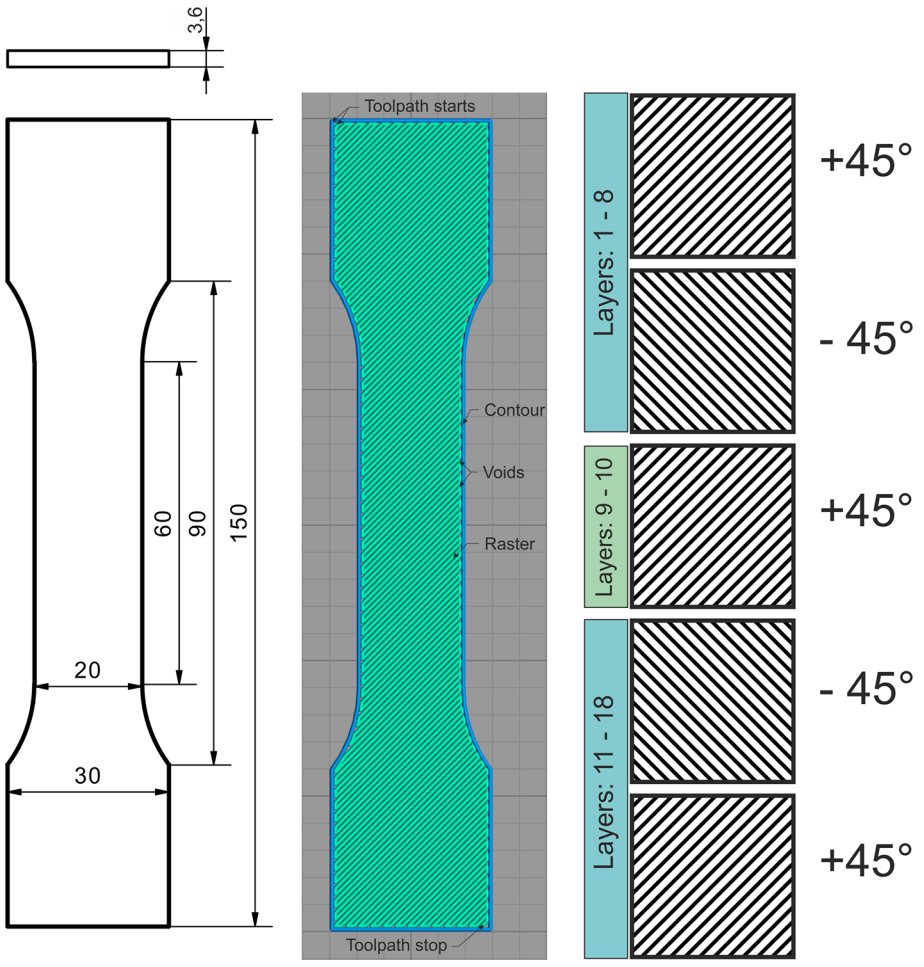


**Figure 1.** Object of research: geometry of specimen, graphical representation of the one layer and graphical representation of the layers in symmetric composite sequence

their initial mechanical strength before aging with various factors.

In paths 2 to 4, PLA and PLA+CF specimens were measured to determine their mechanical strength after aging with various chemical factors, such as buffered saline solution environment (PBS), sterilisation with ethylene oxide (EtO), sterilisation with gas plasma (VH2O2) or both sterilisation with one selected method and then aging in buffered saline solution environment.

At the end of each testing path the specimens were also analysed using the scanning electron microscopy (SEM) with energy dispersive spectroscopy (EDS) technique. The schematic representation of testing paths and specimen preparation before testing is presented in Figure 2.

### *Environmental aging*

Two types of environmental aging were prepared for this research. One way was aging with sterilisation techniques, such as ethylene oxide sterilisation or gas plasma sterilisation. Process of sterilisation was prepared in a specialised company for sterilisation services and validated, according to the PN-EN ISO 17665 standard. In the process of aging with ethylene oxide sterilisation, the following parameters were defined: gas concentration: 450 mg/l; temperature: 55 °C; exposure time: 60 min. Then, after the exposure to the sterilising agent, the specimens were subjected to a degasification period lasting 12 hours in the steriliser chamber. In turn, in the process of aging with gas plasma sterilisation, the following parameters were defined: vapour pressure: 1.9 mm/Hg; temperature: 40 °C; exposure time: 30 min. Each specimen was delivered for further testing enclosed in special packaging for sterilisation.

The second way of aging was aging in buffered saline solution environment. For the aging studies, buffered saline solution (PBS, BIOCORP Poland), pH = 7.2, was used. The specimens were stored in single plastic containers in laboratory dryer at temperature 37 ± 1 °C. The time of aging was divided into three intervals of 1, 6, 12 weeks, marked as W1, W6, W12. The specimens were tested after a fixed exposure time. Also, the pH value of the aging medium was monitored during the test using a pH and conductivity meter. The medium was replaced in all of the containers at every four weeks, before each change, the pH value was measured.

The relative mass change of the specimens during degradation ($\Delta m$) was calculated using the data obtained from the weighing process. The initial mass ($m_0$) of each specimen was measured before placement in the degradation medium, and

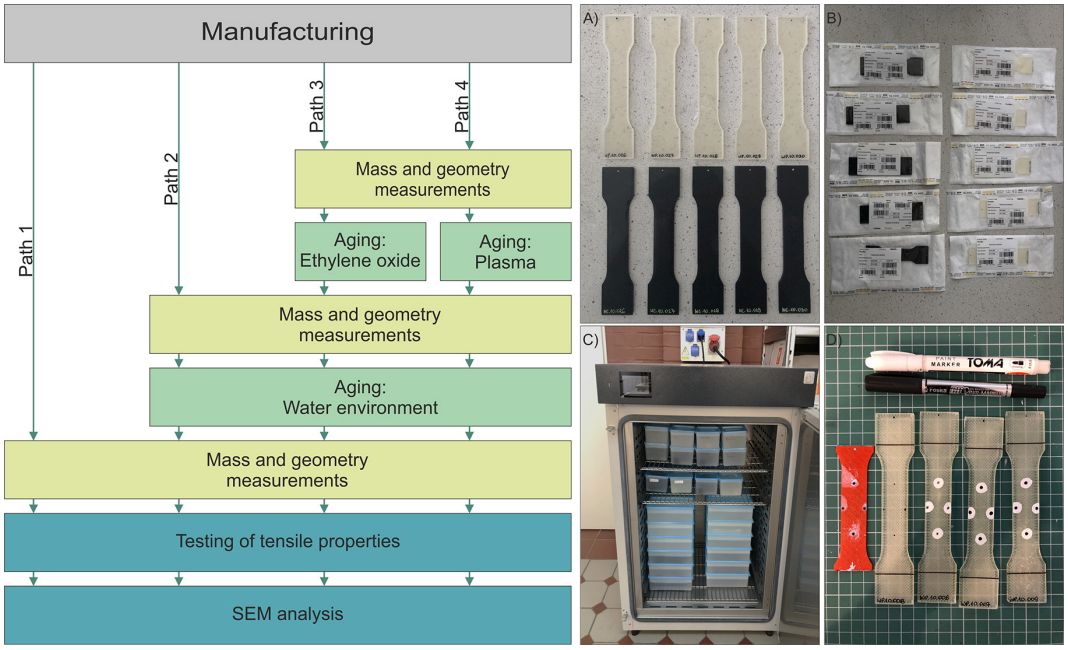


**Figure 2.** Schematic representation of testing procedure for four testing paths (left) and preparation of specimens (right): (a) pure PLA and PLA with CF specimens after manufacturing; (b) specimens wrapped after sterilisation; (c) specimens stored in a medium in a dryer; (d) steps of marking samples for measurement with video-extensometer

the mass at a given time ($m_t$) was noted after a specific degradation period. The mass change was computed using the formula:

$$\Delta m = (m_t - m_0)/ m_0 \times 100\% \quad (1)$$

*Testing equipment*

The mass and geometry of the specimens was measured before aging with sterilisation methods and after them and then before and after aging in a buffered saline solution environment or only before mechanical testing, when the specimens were not aged. The mass of specimens were measured with a Radwag AS 220.X2 PLUS analytical balance (Radwag, Radom, Poland) with precision $d$ = 0.0001 g. The geometry was verified using a micrometre.

The measurements of mechanical properties were conducted using a Zwick/Roell Z10 universal testing machine (ZwickRoell GmbH & Co. KG, Ulm, Germany) equipped with a video-extensometer. The gauge points were marked with a custom made template fabricated on a 3D printer. An initial load of 10 N was applied in the tests. The specimens were loaded to failure with a constant speed of 1 mm/min of the upper crosshead.

After mechanical testing, the fracture surfaces of chosen specimens were evaluated by Hitachi SU3500 Scanning Electron Microscope (Hitachi, Ltd., Tokyo, Japan). It was used to determine fracture surface parameters, such as voids, fibre pull-out and delamination.

*Statistical analysis*

To evaluate the results, the statistical analysis was prepared. The normality of the distribution, the coefficient of variation, and the statistical significance of the differences between the specified parameters were resolved. To evaluate the normality of the distribution of quantitative variables, the Shapiro-Wilk test was used. Verification was provided at a significance level of $\alpha$ = 0.05. Also, the coefficient of variation of the results V was determined for the above-mentioned parameters. It was supposed that achieving a V-ratio of less than 10% means low variability of the feature and, at the same time, non-variability of the examined population.

The statistical significance of the differences in the results was determined using one-way ANOVA. These served to verify the hypothesis of equality of the means of the variable under study in several populations ($k \geq 2$). In addition, Fisher's least significant difference (LSD) post-hoc test was performed. The significance coefficient $\alpha$ = 0.05 was used to check the above parameters, giving the possibility of determining statistically significant differences at $p < 0.05$.

## RESULTS OF MECHANICAL PROPERTIES TESTS

### Pure polylactide vs. polylactide with short carbon fibres reinforcement

The tensile properties were calculated in accordance to the ISO 527 standard [35]. To calculate stress and strain, the values of applied loads and measured strains were collected. A video-extensometer was used to measure strains in longitudinal and transverse directions. Calculation of Young modulus and Poisson ratios was carried out via approximation of stress values derived at strains of $\varepsilon_1$ = 0.05% and $\varepsilon_2$ = 0.25%.

The energy absorbed by the material before specimen failure (toughness) was also determined. The parameter described by relation Equation 2 was determined from the surface under the curve of the monotonic tensile test.

$$Q = \int_t \sigma \, d\varepsilon \quad (2)$$

The stress-strain curves of the representative specimens fabricated with PLA and PLA+CF are presented in Figure 3. The curves obtained for each measured specimen were post-processed ant the mean values of the mechanical properties are collected in Table 1. For the comparison of PLA and PLA+CF, the mean values marked as W0, are specimens non-aged in the buffered saline solution environment.

The tensile curves presented indicate that the mechanical characteristics of PLA and PLA+CF composites evolve with the duration of conditioning in PBS. For pure PLA, the curves exhibit typical brittle material behaviour at weeks W0, W1, and W12, with a more pronounced brittle nature at W6. In contrast, the PLA+CF composites demonstrate stronger, non-ductile characteristics at weeks W0, W1, and W12 (for non-sterilised PLA+CF), while the remaining curves for PLA+CF specimens aged at W6 and W12 show a shift towards ductile material behaviour. This shift indicates that the incorporation of carbon

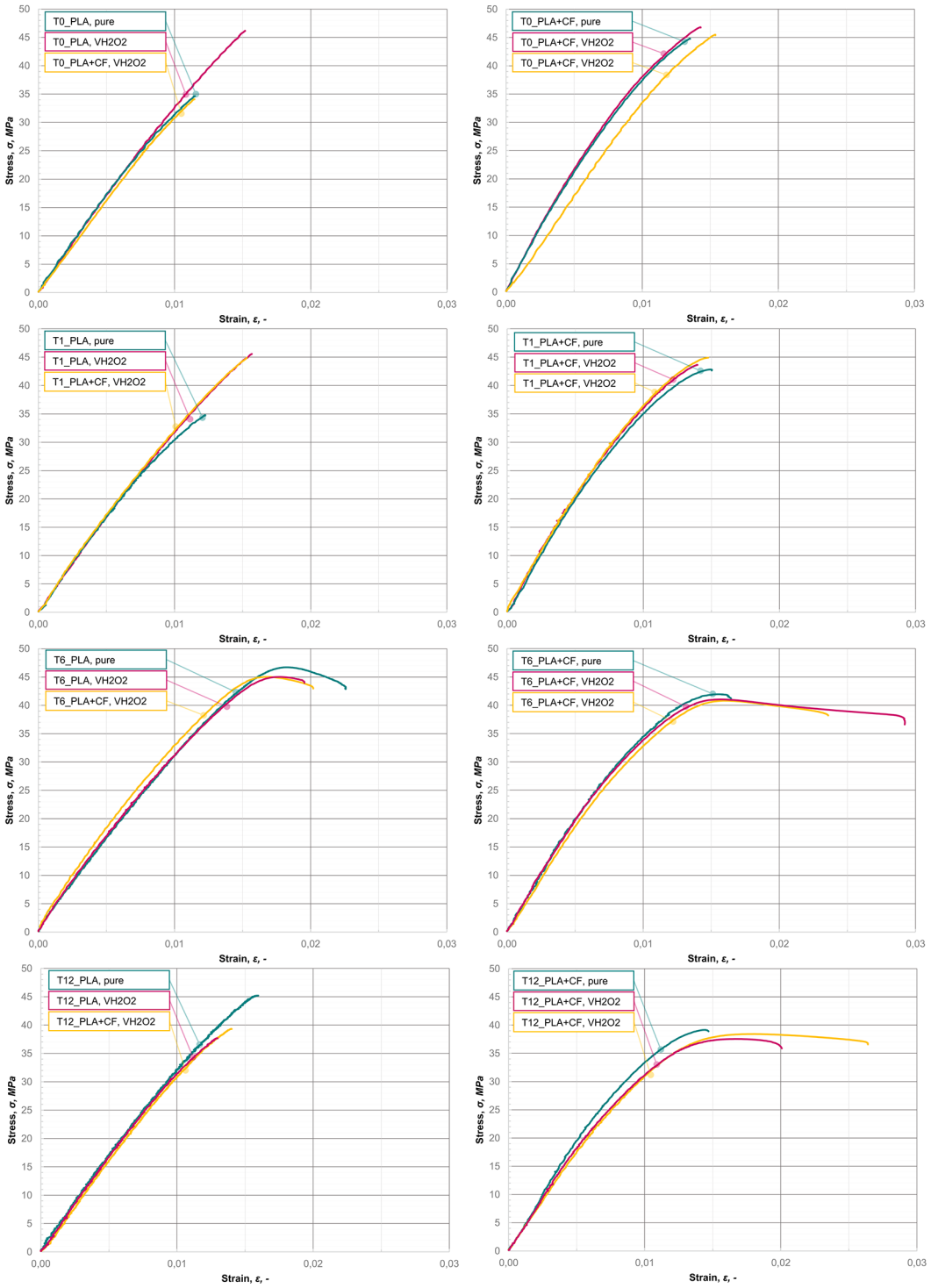


**Figure 3.** Stress-strain curves for PLA and PLA+CF before and after environmental aging in W1, W6, W12

fibres influences the ability of the material to maintain strength and ductility over extended exposure to PBS, particularly in the case of aging with sterilisation agents.

From the results presented in Table 1, it can be observed that the tensile strength of PLA+CF specimens was, on average, 1.38 times higher than that of PLA specimens when no aging agents were applied. For specimens aged with ethylene oxide (EtO) or gas plasma (VH2O2), the tensile strength of PLA+CF specimens was 1.41 and 1.06 times higher than that of PLA specimens, respectively. A two-sample t-test confirmed that these differences were statistically significant, with a p-value of $< 0.0001$. An analysis of the differences in Young's modulus revealed that the values for

**Table 1.** Summaries of tensile strength, tensile modulus, Poisson ratio, toughness and mass change for each PLA and PLA+CF, n = 5, mean with standard deviation

| Week, W | Non-aged | | Aged with ethylene oxide (EtO) | | Aged with plasma (VH2O2) | |
|---|---|---|---|---|---|---|
| | PLA | PLA+CF | PLA | PLA+CF | PLA | PLA+CF |
| Tensile strength, $\sigma_m$ (MPa), *n*=5 | | | | | | |
| W0 | 31.71 ± 2.07 | 43.88 ± 0.88 | 31.69 ± 1.97 | 44.88 ± 1.11 | 42.72 ± 4.52 | 45.06 ± 1.52 |
| W1 | 32.03 ± 1.74 | 42.21 ± 0.76 | 42.17 ± 1.66 | 44.09 ± 0.55 | 42.67 ± 3.59 | 42.82 ± 1.11 |
| W6 | 45.47 ± 0.89 | 41.27 ± 0.42 | 44.90 ± 0.14 | 40.16 ± 0.71 | 44.71 ± 0.35 | 40.69 ± 0.31 |
| W12 | 44.41 ± 0.57 | 38.89 ± 0.27 | 37.97 ± 1.00 | 37.45 ± 0.94 | 35.99 ± 2.65 | 36.62 ± 1.01 |
| Young modulus, *E* (MPa), *n*=5 | | | | | | |
| W0 | 4223.47 ± 47.27 | 4711.57 ± 47.12 | 4109.07 ± 201.13 | 4344.95 ± 687.70 | 4268.10 ± 73.14 | 4789.69 ± 80.39 |
| W1 | 4116.46 ± 71.45 | 4522.88 ± 29.04 | 4071.15 ± 76.45 | 4801.22 ± 340.73 | 4118.69 ± 142.00 | 4847.53 ± 50.21 |
| W6 | 3812.52 ± 97.75 | 4589.82 ± 63.62 | 3895.41 ± 94.35 | 4531.19 ± 134.89 | 3755.53 ± 58.14 | 4622.23 ± 76.21 |
| W12 | 3864.95 ± 189.02 | 4559.40 ± 34.54 | 4131.16 ± 177.42 | 3831.03 ± 81.04 | 4095.30 ± 62.31 | 4096.17± 175.55 |
| Poisson ratio, *v* (-), *n*=5 | | | | | | |
| W0 | 0.40 ± 0.02 | 0.44 ± 0.03 | 0.38 ± 0.08 | 0.33 ± 0.11 | 0.41 ± 0.02 | 0.42 ± 0.03 |
| W1 | 0.39 ± 0.03 | 0.44 ± 0.02 | 0.43± 0.04 | 0.44 ± 0.04 | 0.44 ± 0.02 | 0.42 ± 0.02 |
| W6 | 0.43 ± 0.06 | 0.43 ± 0.04 | 0.45 ± 0.10 | 0.46 ± 0.04 | 0.38 ± 0.06 | 0.46 ± 0.01 |
| W12 | 0.45 ± 0.17 | 0.47 ± 0.02 | 0.50 ± 0.12 | 0.43 ± 0.05 | 0.44 ± 0.04 | 0.44 ± 0.08 |
| Toughness, $U_T$ (MJ/m$^3$), *n*=5 | | | | | | |
| W0 | 0.17 ± 0.02 | 0.28 ± 0.01 | 0.19 ± 0.02 | 0.34 ± 0.06 | 0.34 ± 0.07 | 0.29 ± 0.02 |
| W1 | 0.19 ± 0.03 | 0.27 ± 0.02 | 0.34 ± 0.03 | 0.31 ± 0.03 | 0.34 ± 0.06 | 0.29 ± 0.02 |
| W6 | 0.35 ± 0.02 | 0.21 ± 0.05 | 0.33 ± 0.03 | 0.15 ± 0.08 | 0.35 ± 0.03 | 0.12 ± 0.07 |
| W12 | 0.37 ± 0.02 | 0.19 ± 0.04 | 0.26 ± 0.02 | 0.15 ± 0.06 | 0.24 ± 0.03 | 0.19 ± 0.03 |
| Mass change, Δ*m, (*%), *n*=5 | | | | | | |
| W0 | x | x | x | x | x | x |
| W1 | 0.60 ± 0.01 | 0.64 ± 0.04 | 0.62 ± 0.01 | 0.57 ± 0.00 | 0.61 ± 0.01 | 0.59 ± 0.01 |
| W6 | 0.74 ± 0.03 | 0.74 ± 0.02 | 0.74 ± 0.01 | 0.79 ± 0.00 | 0.69 ± 0.02 | 0.71 ± 0.02 |
| W12 | 0.71 ± 0.08 | 1.00 ± 0.02 | 0.78 ± 0.05 | 0.99 ± 0.06 | 0.68 ± 0.08 | 0.98 ± 0.06 |

PLA+CF specimens were 1.05–1.12 times higher than those for PLA specimens. These differences were also statistically significant, with a *p*-value of < 0.0001. Regarding the Poisson's ratio, PLA+CF specimens exhibited higher values than PLA specimens for both non-aged specimens and those aged with VH2O2. However, for the specimens aged with EtO, PLA specimens showed higher Poisson's ratio values. The differences ranged from 1.02 to 1.15 times higher and were statistically significant, with a *p*-value of 0.0190.

In terms of material toughness, PLA+CF specimens demonstrated 1.66 times higher toughness than PLA specimens in the non-aged condition and 1.80 times higher toughness when aged with EtO. Conversely, when aged with VH2O2, PLA specimens exhibited 1.16 times higher toughness than PLA+CF specimens. These differences were statistically significant, with a *p*-value of < 0.0001.

## Pure polylactide aged with sterilisation agents or buffered saline solution environment

The stress-strain curves of representative PLA specimens aged with sterilisation agents and in a buffered saline solution (PBS) environment are shown in Figure 3. These curves, as described earlier, were used to analyse the mechanical properties of the specimens. The analysis of differences between specimen groups was conducted following the testing procedure outlined in Figure 2.

In the second pathway, specimens that were not aged with sterilisation agents were examined. These specimens were aged solely in PBS for durations of one week (W1), six weeks (W6), or twelve weeks (W12). The results were then compared to dry specimens, as discussed in section "Pure Polylactide vs. Polylactide with Short Carbon Fiber Reinforcement."

Aging in PBS was observed to increase the tensile strength of pure PLA specimens. Specifically, the tensile strength for the specimens aged for six (W6) and twelve weeks (W12) was approximately 1.4 times higher than for the specimens at week zero (W0). In contrast, the tensile strength for the specimens aged for one week (W1) was similar to that of W0 specimens. ANOVA analysis indicated that these differences were statistically significant, with a $p$-value of < 0.0001 for comparisons between W0 and W6, W0 and W12, W1 and W6, and W1 and W12.

However, comparisons between W0 and W1 or W6 and W12 revealed no statistically significant differences, with $p$-values of 0.7328 and 0.2655, respectively.

Although the tensile strength values for the specimens aged in PBS were higher than those for the specimens not aged with any agents, the Young's modulus exhibited a different trend. The modulus was highest for specimens in W0 and decreased progressively with longer aging periods. For the W1 specimens, the modulus was the same as in W0, whereas for the W6 and W12 specimens, it was approximately 1.10 times lower than in W0. The differences were statistically significant for comparisons between W0 and W6, W0 and W12, W1 and W6, and W1 and W12, with $p$-values of < 0.0001, < 0.0001, 0.0007, and 0.0032, respectively. However, no statistically significant differences were observed for comparisons between W0 and W1 or W6 and W12, with $p$-values of 0.1596 and 0.4803, respectively.

The Poisson's ratio values remained consistent, indicating that aging in PBS did not significantly alter the transverse deformation of the specimens. Statistically non-significant differences were observed in all comparisons, including W0 vs. W1, W0 vs. W6, W0 vs. W12, W1 vs. W6, W1 vs. W12, and W6 vs. W12, with p-values of 0.9323, 0.5743, 0.7470, 0.5188, 0.6840, and 0.8094, respectively.

Toughness values were approximately twice as high for the specimens aged in PBS for six (W6) or twelve weeks (W12) compared to those in W0 or W1. The toughness values for the W0 and W1 specimens were nearly identical. ANOVA analysis confirmed that the differences were statistically significant for comparisons between W0 and W6, W0 and W12, W1 and W6, and W1 and W12, with $p$-values of < 0.0001 for all. However, comparisons between W0 and W1 or W6 and W12 showed no statistically significant differences, with p-values of 0.0861 and 0.1502, respectively.

In the third and fourth paths, the specimens aged with sterilisation agents were analysed. These specimens, after sterilisation with EtO or VH2O2, were aged in PBS for the same durations as the specimens described previously. For the specimens aged with EtO and PBS, the tensile strength was approximately 1.2 to 1.4 times higher over the aging period corresponding to the buffered saline solution environment compared to dry specimens aged only with EtO. ANOVA analysis showed that these differences were statistically significant, with $p$-values of < 0.0001 for comparisons between W0 and W1, W0 and W6, W0 and W12, and W6 and W12. Statistically significant differences were also found between W1 and W6, and between W1 and W12, with p-values of 0.0066 and 0.0002, respectively.

However, the changes in Young's modulus for the specimens aged with EtO and subsequently aged in PBS followed a pattern similar to that observed for the specimens aged only in PBS. Specifically, the modulus values for the dry specimens aged with EtO were higher than those of the specimens aged in PBS after EtO sterilisation. Statistically non-significant differences were found for comparisons between W0 and W1, W0 and W12, W1 and W6, and W1 and W12, with $p$-values of 0.6892, 0.8155, 0.0774, and 0.5283, respectively. In contrast, statistically significant differences were observed between specimens at W0 and W6, as well as between W6 and W12, with $p$-values of 0.0356 and 0.0222, respectively.

In contrast to the specimens that were not aged with any sterilisation agents, the specimens aged with EtO exhibited changes in Poisson's ratio, with a noticeable decrease over time. The highest Poisson's ratio, 1.32 times greater than that of dry specimens (W0), was observed in the specimens aged in PBS for 12 weeks (W12). For the specimens aged for one (W1) and six weeks (W6), the Poisson's ratio was 1.13 to 1.18 times higher than for dry specimens. The differences were statistically non-significant in comparisons between W0 and W1, W0 and W6, W0 and W12, W1 and W6, W1 and W12, and W6 and W12, with $p$-values of 0.3889, 0.2252, 0.0589, 0.7119, 0.2678, and 0.4512, respectively.

The toughness of specimens aged with EtO and PBS was approximately 1.7 times higher for those aged for one or six weeks (W1 and W6), and about 1.4 times higher for those aged for twelve weeks

(W12), compared to the dry specimens aged only with EtO. Statistically non-significant differences were found between the specimens aged for one and six weeks ($p$-value 0.8186). However, statistically significant differences were observed in comparisons between W0 and W1, W0 and W6, W0 and W12, W1 and W12, and W6 and W12, with $p$-values of < 0.0001 for the first two comparisons, and 0.0005, 0.0001, and 0.0002 for the others.

When the sterilising agent was changed to VH2O2, the tensile strength of the specimens aged in PBS for one and six weeks (W1 and W6) remained similar to that of the dry specimens. However, the specimens aged in PBS for twelve weeks (W12) had 1.2 times lower tensile strength than the dry specimens.

The changes in Young's modulus followed a similar pattern to those observed in the specimens aged with EtO. Additionally, the changes in Poisson's ratio and toughness for the specimens aged with VH2O2 before aging in PBS were similar to those observed in the specimens aged with EtO, with comparable trends over the aging period in PBS.

### Polylactide with short carbon fibres reinforcement aged with sterilisation agents or buffered saline solution environment

Aging in PBS resulted in higher tensile strength values for PLA+CF specimens. The tensile strength was approximately 1.3 times higher at W1, 1.4 times higher at W6, and 1.2 times higher at W12 compared to W0. ANOVA analysis revealed that these differences were statistically significant, with $p$-values of < 0.0001 for comparisons between W0 and W6, W0 and W12, W1 and W12, and W6 and W12. For other comparisons, the p-values were 0.0007 (W0 and W1) and 0.0308 (W1 and W6).

Despite the higher tensile strength values for specimens aged in PBS compared to non-aged specimens, the Young's modulus was 1.3 times higher for the W0 specimens and decreased with longer aging. Statistically significant differences were found in comparisons between W0 and W1, W0 and W6, W0 and W12, and W1 and W6, with $p$-values of < 0.0001, 0.0006, < 0.0001, and 0.0337, respectively. However, no statistically significant differences were observed between W1 and W12, or W6 and W12, with $p$-values of 0.2232 and 0.3068, respectively. Poisson's ratio remained consistent across all aging periods, indicating that aging in PBS did not substantially affect the transverse deformation of the PLA+CF material. Toughness values were approximately 1.47 times higher for the specimens aged for twelve weeks (W12) compared to non-aged specimens (W0), and 1.30 times higher in W0 compared to the specimens aged for six weeks (W6). The toughness values for W0 and W1 specimens were nearly identical. The differences between groups were not statistically significant.

The toughness values were approximately 1.08 to 1.16 times higher for non-aged specimens compared to those aged in PBS for six or twelve weeks. Meanwhile, the toughness values for non-aged specimens (W0) and those aged for one week (W1) were nearly identical. Statistically significant differences were observed in comparisons between W0 and W6, W0 and W12, W1 and W6, and W1 and W12, with $p$-values of 0.0075, 0.0007, 0.0285, and 0.0029, respectively.

In the third and fourth paths, the PLA+CF specimens aged with sterilisation agents were evaluated. These specimens were sterilised using either EtO or VH2O2 and subsequently aged in PBS for the same durations as described for the previous specimens.

The specimens aged with EtO and subsequently in PBS exhibited tensile strength values approximately 1.2 times higher throughout the aging weeks in PBS compared to the dry specimens aged only with EtO. Statistically significant differences were observed in comparisons between W0 and W6, W0 and W12, W1 and W6, and W1 and W12, with $p$-values < 0.0001. For the comparison between W6 and W12, the p-value was 0.0006.

Regarding changes in Young's modulus for the specimens aged with EtO and then in PBS, the trend mirrored that observed in the specimens aged only in PBS (without prior sterilisation). The Young's modulus values of dry specimens aged with EtO were higher than those of the specimens further aged in PBS. Statistically significant differences were identified in comparisons between W0 and W12, W1 and W6, W1 and W12, and W6 and W12, with $p$-values of < 0.0001, 0.0491, 0.0408, and < 0.0001, respectively.

The specimens aged with EtO showed no significant changes in Poisson's ratio, consistent with the results observed for specimens not subjected to sterilisation. The differences between groups were not statistically significant.

The toughness of PLA+CF specimens aged with EtO and PBS was approximately 1.1 times higher for the specimens aged for one week (W1)

and about 2.2 times higher for the specimens aged for six or twelve weeks (W6 or W12) compared to dry specimens aged only with EtO. Statistically significant differences were observed in comparisons between W0 and W6, W0 and W12, W1 and W6, and W1 and W12, with *p*-values of < 0.0001, 0.0001, 0.0005, and 0.0006, respectively.

When the sterilising agent was changed to VH2O2, the tensile strength values of the PLA+CF specimens were comparable for the specimens additionally aged in PBS over one week (W1). However, the dry specimens exhibited 1.1–1.2 times higher tensile strength than those aged for six weeks (W6) or twelve weeks (W12), respectively. Statistically significant differences were observed in comparisons between W0 and W6, W0 and W12, W1 and W12, and W6 and W12, with *p*-values < 0.0001. Additionally, comparisons between W0 and W1 or W1 and W6 showed *p*-values of 0.0047 and 0.0068, respectively. Unlike the specimens aged only in PBS, differences in Young's modulus were noted for the specimens at W12. The Young's modulus of dry specimens (W0) was approximately 1.07–1.16 times higher than that of the specimens at W6 or W12. However, for W1, the values were nearly identical to those of dry specimens. Statistically significant differences were observed in

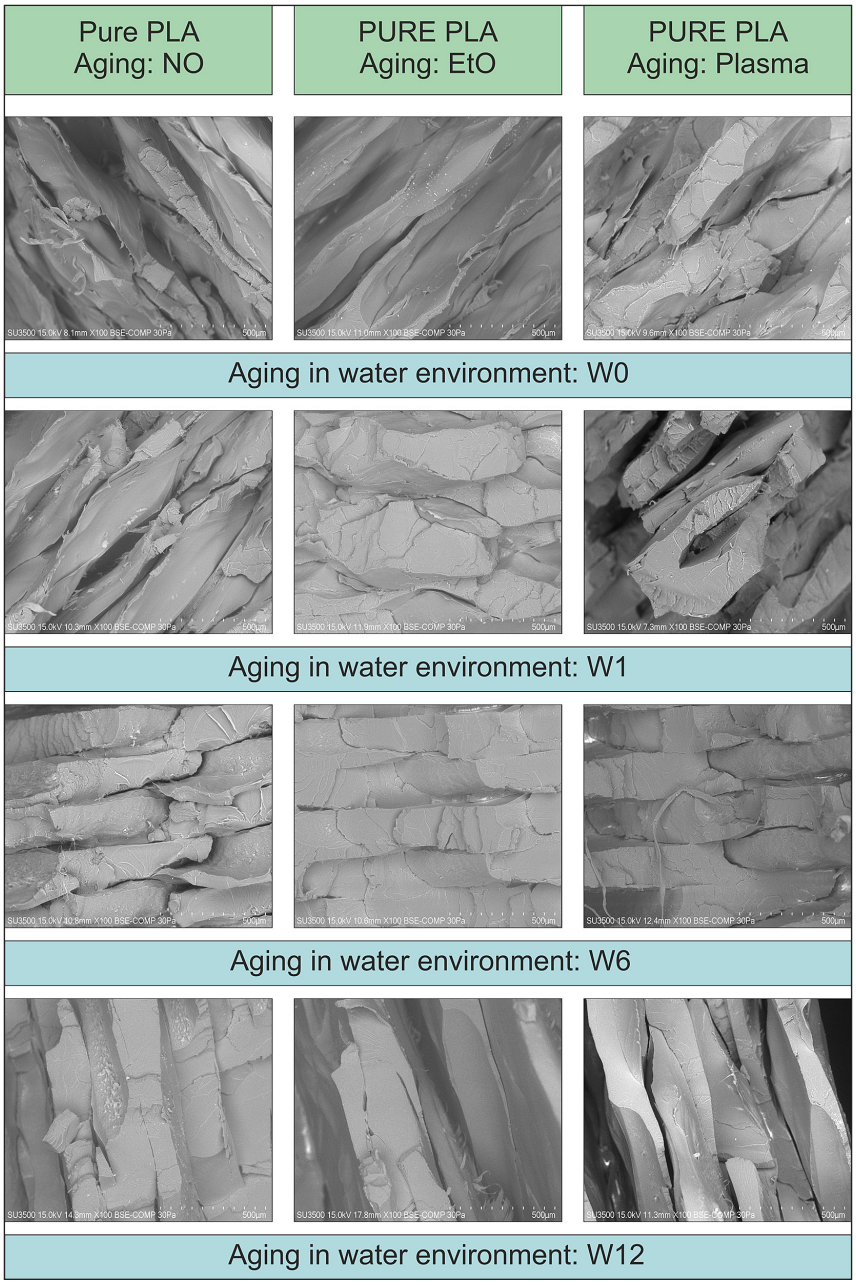


**Figure 4.** SEM image of non-reinforced PLA specimens before and after aging

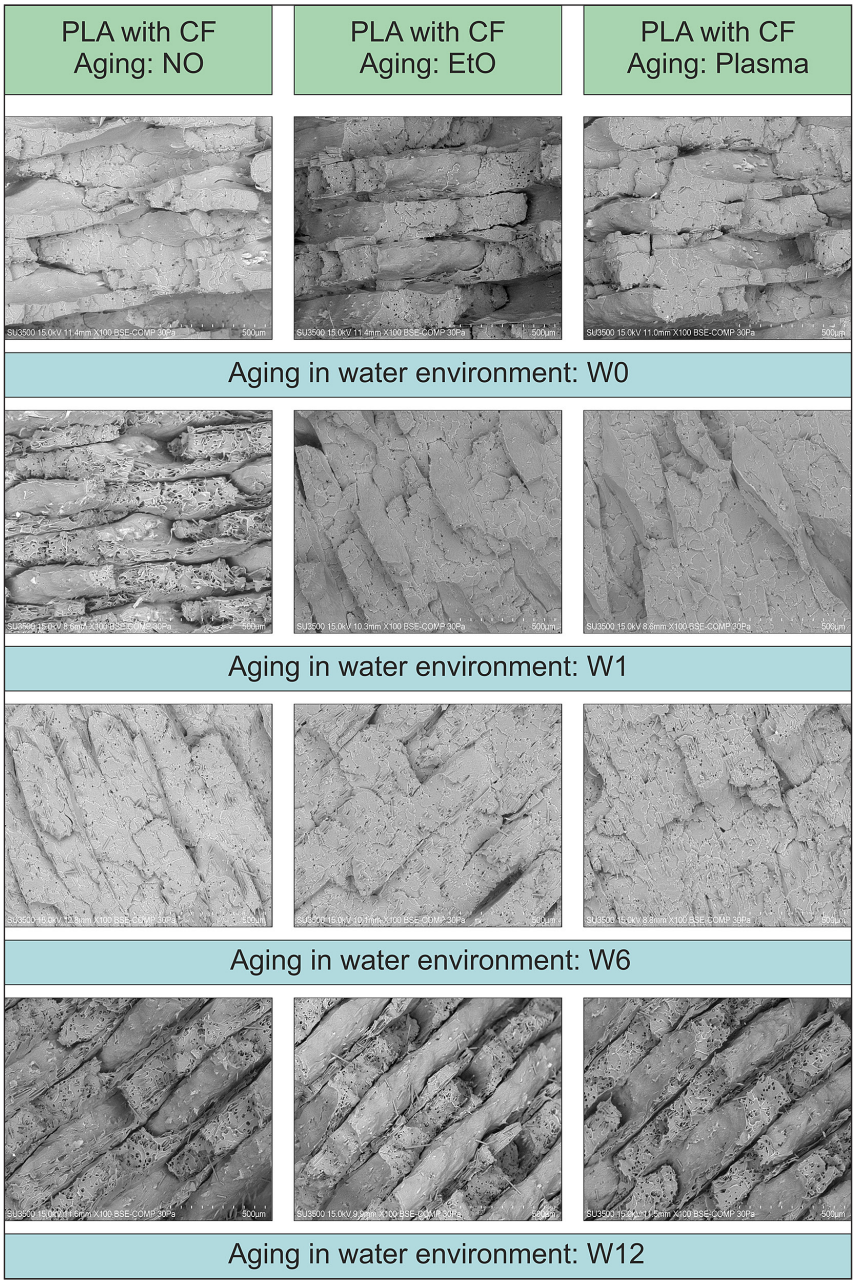


**Figure 5.** SEM image of carbon fibres reinforced PLA specimens before and after aging

comparisons between W0 and W6 ($p$ = 0.0247) and W1 and W6 ($p$ = 0.0042). For comparisons involving W0 and W12, W1 and W12, and W6 and W12, the $p$-value was < 0.0001. For the specimens aged with VH2O2 prior to aging in PBS, the Poisson's ratio remained largely unchanged over the aging period. The differences between groups were not statistically significant. The toughness values of PLA+CF specimens varied with aging time. For dry specimens (W0), toughness was approximately 1.5–2.5 times higher than for the specimens aged for six weeks (W6) or twelve weeks (W12). For the W1 specimens, toughness was similar to that of dry specimens. Statistically significant differences were observed in comparisons between W0 and W6 and W1 and W6 ($p$ < 0.0001). Comparisons between W0 and W12, W1 and W12, and W6 and W12 yielded $p$-values of 0.0011, 0.0010, and 0.0080, respectively.

## MICROGRAPHY OF PLA AND PLA+CF SPECIMENS

Figures 4 to 5, present the SEM images of the fracture surfaces for materials considered in this study. The images in the first row represents the

fracture surfaces of the PLA or PLA+CF before aging in PBS. Each column represents the fracture surfaces at different aging factors, wherein the first column presents the specimens not subjected to aging, the second column presents the fracture surfaces after aging with EtO and the last column presents the fracture surfaces after aging with VH2O2. Correspondingly, further rows present the fracture surfaces after aging with PBS over W1, W6 or W12 weeks of soaking. In each specimen, details of the printing process, especially the cross-sectional shape of the raster lines and voids between them, can be observed (see Figures 4 and 5).

Figure 4 shows the fractures of single PLA lines where in its cross-section or in its side are marked stress whitening (crazing), associated with brittle characteristic of material which was pre*sented* in Figure 3. This applies to the effect of fibre-reinforced thermoplastic composite materials, in which the fibres and matrix are deformed under tensile loading. By the time the composite material deforms at a certain rate, the fibres can be pulled out of the matrix rather than completely broken off. This causes the composite material to appear visually whiter and less transparent, since pulled fibres scatter light differently than intact composite. The phenomenon of fibre pullout during tensile deformation has been widely reported and studied in the literature on the failure mechanisms of fibre-reinforced composites [35]. On the other hand, Figure 5 shows crazes with failed fibrils, especially in W6 and W12, associated with more ductile characteristic of material than in the case of pure PLA.

Moreover Figure 5 shows small circular voids (black dots) in the PLA matrix, these voids have the same shape as the short carbon fibre and it should be places of pulled out fibres. Also, in Figure 5, single carbon fibres can be observed; especially, they are illustrated in fracture surfaces corresponding to time of PBS aging marked as W6 and W12. On the basis of fracture surfaces, it can be observed that the orientation of short carbon fibre in polymer in general respond to the feeding direction, and the 3D printed material should be classified as unidirectional fibre-reinforced composites.

## CONCLUSIONS

This study investigated the mechanical properties and failure modes of non-reinforced PLA and carbon fibre-reinforced PLA (PLA+CF) specimens processed using Fused Filament Fabrication (FFF), with a focus on the impact of environmental aging. The specimens, printed with a symmetrical laminate orientation [+45°/-45°], were subjected to aging in a buffered saline solution and sterilisation agents over one, six, or twelve weeks, and compared to non-aged specimens.

The results show that carbon fibre reinforcement significantly improves the tensile strength, modulus, and toughness of PLA+CF compared to pure PLA. However, the adhesion between the carbon fibres and the polymer matrix remains a potential issue, with SEM micrographs indicating that fibre pullout, rather than fibre breakage, is the primary failure mode during tensile testing. This observation suggests that the bond between the fibres and the matrix may not be fully optimised, potentially limiting the overall mechanical performance of the composite.

Additionally, aging in both sterilisation agents and buffered saline solution had a notable effect on the mechanical properties of PLA+CF. Sterilised specimens exhibited higher toughness than their non-aged counterparts, but when further exposed to the buffered saline solution, a dramatic reduction in toughness was observed, particularly in fibre-reinforced specimens. In contrast, non-reinforced PLA showed less deterioration in toughness, highlighting the accelerated aging effect in fibre-reinforced polymers. This phenomenon suggests that moisture absorption, when combined with other aging factors such as temperature or sterilisation agents, can lead to a faster degradation of mechanical properties. Similar effects have been observed in other composite systems, such as carbon fibre-reinforced polyamide.

Overall, while carbon fibre reinforcement provides a clear enhancement in mechanical strength, it may not be suitable for applications where the material is exposed to harsh environmental conditions for extended periods.

The accelerated loss of fracture toughness observed under certain conditions, particularly when exposed to moisture and sterilisation agents, significantly impacts the durability and reliability of carbon fibre-reinforced PLA (PLA+CF). This phenomenon can be attributed to several factors, including the compromised interfacial bond between the carbon fibres and the PLA matrix under environmental stress, leading to increased susceptibility to failure. Furthermore, moisture absorption, especially in combination with sterilisation processes, accelerates the degradation of the mechanical properties of the composite, resulting in a

reduced ability to withstand fracture-induced failure. These findings are critical for understanding the long-term behaviour of 3D-printed composites and their performance in real-world applications.

The implications of these results underscore the importance of considering environmental factors when selecting materials for specific applications. While carbon fibre reinforcement enhances strength and stiffness, the degradation of fracture toughness under environmental aging must be factored into the material selection process, particularly for components exposed to harsh or moisture-rich conditions. This study suggests that, for certain high-performance applications where durability under adverse environmental conditions is a priority, carbon fibre-reinforced PLA may not be the optimal material choice unless further optimisation of fibre-matrix bonding and moisture resistance is achieved.

This study highlighted the balance between the mechanical benefits of carbon fibre reinforcement and the limitations imposed by environmental aging, underscoring the need for careful consideration of operational conditions when selecting materials for practical use.

## Acknowledgement

This research was funded by National Science Centre, Poland, DEC-2021/05/X/ST8/00113.

## REFERENCES

1. Komorek A, Bakuła M, Bąbel R, Woziński P, Rośkowicz M. The influence of 3D printing direction on the mechanical properties of manufactured elements. Adv Sci Technol Res J; 2024; 18: 86–95. https://doi.org/10.12913/22998624/193528
2. Hanon, M. M., Alshammas, Y., Zsidai, L. Effect of print orientation and bronze existence on tribological and mechanical properties of 3D-printed bronze/PLA composite, Int. J. Adv. Manuf. Technol., 2020; 108(1–2): 553–570, https://doi.org/10.1007/s00170-020-05391-x
3. Tao Y., Kong F., Li Z., et al. A review on voids of 3D printed parts by fused filament fabrication, J. Mater. Res. Technol., 2021; 15: 4860–4879, https://doi.org/10.1016/j.jmrt.2021.10.108
4. Yao, T., Deng, Z., Zhang K., Li S. A method to predict the ultimate tensile strength of 3D printing polylactic acid (PLA) materials with different printing orientations, Compos. Part B Eng., 2019; 163, January: 393–402, https://doi.org/10.1016/j.compositesb.2019.01.025
5. Zhang, H., Huang, T., Jiang, Q., He, L., Bismarck, A., Hu, Q. Recent progress of 3D printed continuous fiber reinforced polymer composites based on fused deposition modeling: a review, J. Mater. Sci., 2021; (23): 12999–13022, https://doi.org/10.1007/s10853-021-06111-w
6. Chen, Y., Klingler, A., Fu, K., Ye, L. 3D printing and modelling of continuous carbon fibre reinforced composite grids with enhanced shear modulus, Eng. Struct., 2023; 286, No. April: 116165, https://doi.org/10.1016/j.engstruct.2023.116165
7. Srinivasan Ganesh Iyer, S., Keles, O. Effect of raster angle on mechanical properties of 3D printed short carbon fiber reinforced acrylonitrile butadiene styrene, Compos. Commun., 2022; 32, No. April: 101163, https://doi.org/10.1016/j.coco.2022.101163
8. Liu, Z., Lei, Q., Xing, S. Mechanical characteristics of wood, ceramic, metal and carbon fiber-based PLA composites fabricated by FDM, J. Mater. Res. Technol., 2019; 8(5): 3743–3753, https://doi.org/10.1016/j.jmrt.2019.06.034
9. Goh G.D., Dikshit V., Nagalingam A.P., Goh G.L., Agarwala S., Sing S.L., et al. Characterization of mechanical properties and fracture mode of additively manufactured carbon fiber and glass fiber reinforced thermoplastics. Mater Des; 2018; 137: 79–89. https://doi.org/https://doi.org/10.1016/j.matdes.2017.10.021
10. Rossing L., Scharff R.B.N., Chömpff B., Wang C.C.L., Doubrovski E.L. Bonding between silicones and thermoplastics using 3D printed mechanical interlocking. Mater Des; 2020; 186: 108254. https://doi.org/https://doi.org/10.1016/j.matdes.2019.108254
11. Somireddy M., Singh C.V., Czekanski A. Analysis of the material behavior of 3D printed laminates via FFF. Exp Mech; 2019; 59: 871–81. https://doi.org/10.1007/s11340-019-00511-5
12. Bragaglia M., Cecchini F., Paleari L., Ferrara M., Rinaldi M., Nanni F. Modeling the fracture behavior of 3D-printed PLA as a laminate composite: Influence of printing parameters on failure and mechanical properties. Compos Struct; 2023; 322: 117379. https://doi.org/10.1016/j.compstruct.2023.117379
13. llen R.J.A., Trask R.S. An experimental demonstration of effective Curved Layer Fused Filament Fabrication utilising a parallel deposition robot. Addit Manuf; 2015; 8: 78–87. https://doi.org/10.1016/j.addma.2015.09.001
14. Gao X., Qi S., Kuang X., Su Y., Li J., Wang D. Fused filament fabrication of polymer materials: A review of interlayer bond. Addit Manuf; 2021; 37: 101658. https://doi.org/10.1016/j.addma.2020.101658
15. Moetazedian A., Gleadall A., Han X., Silberschmidt V.V. Effect of environment on mechanical properties

of 3D printed polylactide for biomedical applications, J. Mech. Behav. Biomed. Mater., 2019; 102, No. August 2019, 103510, https://doi.org/10.1016/j.jmbbm.2019.103510

16. Hasan M.S., Ivanov, T., Vorkapic M., et al. Impact of aging effect and heat treatment on the tensile properties of PLA (poly lactic acid) printed parts, Mater. Plast., 2020; 57(3), 147–159, https://doi.org/10.37358/MP.20.3.5389
17. Moetazedian, A., Gleadall, A., Han, X., Ekinci, A., Mele, E., Silberschmidt, V.V. Mechanical performance of 3D printed polylactide during degradation, Addit. Manuf., 2020; 38, No. November 2020: 101764, https://doi.org/10.1016/j.addma.2020.101764
18. Sedlak J., Joska E., Jansky J., et al. Analysis of the mechanical properties of 3D-printed plastic samples subjected to selected degradation Effects, Materials (Basel)., 2023; 16(8), https://doi.org/10.3390/ma16083268
19. Amza C.G., Zapciu A., Baciu F., Vasile M.I., Popescu D. Aging of 3d printed polymers under sterilizing uv-c radiation, Polymers (Basel)., 2021; 13(24), 1–16, https://doi.org/10.3390/polym13244467
20. Andrzejewska A. J. Experimental study on the effect of selected sterilization methods on mechanical properties of polylactide FFF specimens, Rapid Prototyp. J., 2022; No. August, https://doi.org/10.1108/RPJ-05-2021-0115
21. Pinho A.C., Piedade A.P. Influence of build orientation, geometry and artificial saliva aging on the mechanical properties of 3d printed poly(ε-caprolactone), Materials (Basel)., 2021; 14(12), https://doi.org/10.3390/ma14123335
22. Chausse V., Iglesias C., Bou-Petit E., Ginebra M.P., Pegueroles, M. Chemical vs thermal accelerated hydrolytic degradation of 3D-printed PLLA/PLCL bioresorbable stents: Characterization and influence of sterilization, Polym. Test., 2023; 117, No. October 2022, https://doi.org/10.1016/j.polymertesting.2022.107817
23. Upadhyay R.K., Mishra A.K., Kumar A. Mechanical degradation of 3D printed PLA in simulated marine environment, Surfaces and Interfaces, 2020; 21, No. October, 100778, https://doi.org/10.1016/j.surfin.2020.100778
24. Chaudhary, B., Li, H., Matos, H. Long-term mechanical performance of 3D printed thermoplastics in seawater environments, Results Mater., 2023; 17, No. February: 100381, https://doi.org/10.1016/j.rinma.2023.100381
25. Jiang D., Smith D. E. Anisotropic mechanical properties of oriented carbon fiber filled polymer composites produced with fused filament fabrication, Addit. Manuf., 2017; 18: 84–94, https://doi.org/10.1016/j.addma.2017.08.006
26. Magri A. El, El Mabrouk K., Vaudreuil S., Touhami M.E. Mechanical properties of CF-reinforced PLA parts manufactured by fused deposition modeling, J. Thermoplast. Compos. Mater., 2021; 34(5): 581–595, https://doi.org/10.1177/0892705719847244
27. Venkatesh, R., Jerold John Britto, J., Amudhan, K., Anbumalar, V., Prabhakaran, R., Thiyanesh Sakthi, R. Experimental investigation of mechanical properties on CF reinforced PLA, ABS and Nylon composite part, Mater. Today Proc., 2023; 76: 647–653, https://doi.org/10.1016/j.matpr.2022.12.091
28. Tian F., Zhong Z. Modeling of load responses for natural fiber reinforced composites under water absorption. Compos Part A Appl Sci Manuf 2019; 125: 105564, https://doi.org/10.1016/j.compositesa.2019.105564
29. Fang, M. et al. Effects of hydrothermal aging of carbon fiber reinforced polycarbonate composites on mechanical performance and sand erosion resistance, Polymers (Basel)., 2020; 12(11), 1–11, https://doi.org/10.3390/polym12112453
30. Bachchan, A. A., Das, P. P., Chaudhary, V. Effect of moisture absorption on the properties of natural fiber reinforced polymer composites: A review, Mater. Today Proc., 2022; 49: 3403–3408, https://doi.org/j.matpr.2021.02.812
31. Al-Maharma, A.Y., Al-Huniti, N. Critical review of the parameters affecting the effectiveness of moisture absorption treatments used for natural composites, J. Compos. Sci., 2019; 3(1), https://doi.org/10.3390/jcs3010027
32. Dhieb H., Buijnsters J.G., Eddoumy F., Vázquez L., Celis J.P. Surface and sub-surface degradation of unidirectional carbon fiber reinforced epoxy composites under dry and wet reciprocating sliding. Compos Part A Appl Sci Manuf; 2013; 55: 53–62. https://doi.org/10.1016/j.compositesa.2013.08.006
33. Luo J.-J., Daniel, I. M. Sublaminate-based lamination theory and symmetry properties of textile composite laminates, Compos. Part B Eng., 2004; 35(6), 483–496, https://doi.org/10.1016/j.compositesb.2003.11.005
34. Dano M.L. and Hyer M.W. "Thermally-induced deformation behavior of unsymmetric laminates," Int. J. Solids Struct., 1998; 35(17), 2101–2120, https://doi.org/10.1016/S0020-7683(97)00167-4
35. International Organization For Standarization, "ISO 527-1:2012 Plastics – Determination of tensile properties – Part 1: General principles." 2012.
36. Ashrafi S.A, Miller P.W, Wandro, K.M., Kim, D. Characterization and effects of fiber pull-outs in hole quality of carbon fiber reinforced plastics composite. Materials (Basel)., 2016; 9: 1–12, https://doi.org/10.3390/ma9100828